OXFORD

The path of dishonesty: identification of mental processes with electrical neuroimaging

Laura K. Globig [ID][1,2,3,*,†], Lorena R.R. Gianotti [ID][1,*,†], Giorgia Ponsi [ID][1,4,5], Thomas Koenig [ID][6], Franziska M. Dahinden [ID][1], Daria Knoch [ID][1,*]

[1]Department of Social Neuroscience and Social Psychology, Institute of Psychology, University of Bern, Bern 3012, Switzerland,
[2]Affective Brain Lab, Department of Experimental Psychology, University College London, London, WC1H 0AP, United Kingdom,
[3]The Max Planck UCL Centre for Computational Psychiatry and Ageing Research, University College London, London, WC1H 0AP, United Kingdom,
[4]Department of Psychology, Italian Institute of Technology, Sapienza University of Rome and CLN2S@Sapienza, Rome 00185, Italy,
[5]IRCCS Santa Lucia Foundation, Rome 00170, Italy,
[6]Translational Research Center, University Hospital of Psychiatry, University of Bern, Bern 3012, Switzerland

*Corresponding authors: Department of Social Neuroscience and Social Psychology, Institute of Psychology, University of Bern, Bern, Switzerland.
Emails: daria.knoch@unibe.ch; laura.globig@gmail.com; lorena.gianotti@unibe.ch
†Laura K. Globig and Lorena R.R. Gianotti shared first authorship

Much research finds that lying takes longer than truth-telling. Yet, the source of this response time difference remains elusive. Here, we assessed the spatiotemporal evolution of electrical brain activity during honesty and dishonesty in 150 participants using a sophisticated electrical neuroimaging approach—the microstate approach. This uniquely positioned us to identify and contrast the entire chain of mental processes involved during honesty and dishonesty. Specifically, we find that the response time difference is the result of an additional late-occurring mental process, unique to dishonest decisions, interrupting the antecedent mental processing. We suggest that this process inhibits the activation of the truth, thus permitting the execution of the lie. These results advance our understanding of dishonesty and clarify existing theories about the role of increased cognitive load. More broadly, we demonstrate the vast potential of our approach to illuminate the temporal organization of mental processes involved in decision-making.

Key words: dishonesty; ERP; electrical neuroimaging; microstates; response times.

Introduction

The average person lies at least once a day (e.g. DePaulo 2004). Many of these lies are self-serving and subsequentially detrimental to others: The telling of the lie results in a win for oneself and a loss for the other. Such dishonest behavior has had a dramatic impact on economics, policy, and education (e.g. Mauro 1995; Tanzi and Davoodi 1998; Heyneman et al. 2008). Unsurprisingly, therefore, a large body of research spanning psychology and economics as well as communication and security studies has sought to understand the topic of dishonesty more precisely (e.g. Abe et al. 2006; Engelmann and Fehr 2016; Gächter and Schulz 2016; Maréchal et al. 2017; Speer et al. 2020). A recurrent finding in the literature is that lying takes longer than truth-telling (for an overview, see Suchotzki et al. 2017, but, see Shalvi et al. 2012). However, as yet, we lack a comprehensive understanding of why this is case.

Longer response times are thought to be indicative of more effortful, cognitively demanding processes (Kahneman 2011, but, see e.g. Kruglanski and Gigerenzer 2011). In line with this, much of the previous literature argues that lying requires more cognitive resources, effort, and deliberation than truth-telling (e.g. Zuckerman et al. 1981; Sporer and Schwandt 2006, 2007; Vrij et al. 2010; Walczyk et al. 2014; Debey et al. 2015). But how this increased demand for cognitive resources precisely manifests is still unclear. It seems plausible that lying takes longer than truth-telling because of 2 possible explanations. First, it could be that an additional mental process, such as response inhibition, is required to prevent a prepotent honest response. A second, nonmutually exclusive possibility is that while the same mental processes may be performed in both conditions, 1 or multiple processes could necessitate more time, reflecting prolonged, more elaborate cognitive processes during dishonesty.

To tease apart which or if any of these 2 explanations can account for the observed response time effect, it is necessary to identify and time the entire chain of mental processes involved in both truth- and lie-telling. Mental processes are mediated by large-scale neural networks linking groups of neurons in separate cortical areas into functional entities (e.g. Bressler 1995; Mesulam 1998; Fuster 2006). The activity in these neural networks can be studied with millisecond resolution using the spatiotemporal analysis of multichannel EEG. By segmenting electrical activity recorded during the execution of a task into time periods of stable neural network configurations, one can identify the functional microstates of the brain that each represent the implementation of a specific mental process (e.g. Lehmann and Skrandies 1980; Michel et al. 1993). Capitalizing on such an integrative analysis of space and time information of event-related potential (ERP) data, the microstate approach thus allows us to identify all mental processes involved during spontaneous self-serving dishonest and honest behavior and to determine their order of appearance.

Here, we analyzed data from 150 participants who played an ecologically valid, 2-player card game paradigm in which they

were free to lie to their opponent about the outcome (a schematic representation and description of the experimental task is shown in Fig. 1). To mimic real-world scenarios, decisions were potentially detrimental, resulting in either a loss or a win for the participants and their opponents, spontaneous, that is, to say participants received no instruction to lie, and entirely anonymous. To isolate what distinguishes both actions on a neural and behavioral level, we contrast spontaneously occurring self-serving dishonesty with spontaneously occurring self-serving honesty in order to understand the evolution of cognitive processes involved when the outcome of the participant's response is the same—a win for the participant and a loss for their opponent.

By combining a data-driven, spatiotemporal EEG microstate analysis approach with an ecologically valid 2-player paradigm, we are able to reveal the cause of the observed response time differences. Moreover, we localized the intracranial brain sources underlying each mental process to estimate which brain areas were activated during spontaneous self-serving honest and dishonest behavior.

Materials and methods
Participants

We collected data from 150 participants recruited from the University of Bern. They provided written informed consent and were informed of their right to discontinue participation at any time. The study was approved by the local ethics committee and was conducted in accordance with the declaration of Helsinki. All participants were right-handed, German-speaking and indicated neither current nor previous history of neurological and psychiatric disorders and alcohol and drug abuse. Two participants were excluded due to technical difficulties, leaving a sample of 148 participants (99 females and 49 males; age: M = 21.2 years; SD = 3.0 years, range: 18–30 years). Participants were remunerated with a flat fee of 25 Swiss francs (CHF 1 ≈ USD 1) in addition to the money earned in the behavioral task.

Dishonesty task

The "temptation to lie" game, a computerized 2-player card game (Panasiti et al. 2011, 2014, 2016; Azevedo et al. 2018) was used to study spontaneous dishonesty. Participants took the role of the agents and played against real anonymous interaction partners who took the role of the recipients.

In each trial, 2 cards, the ace of hearts (the winning card, worth CHF 9) and the ace of spades (the losing card, worth CHF 0) were presented horizontally. The recipient, who had been presented with the 2 cards face-down, blindly assigned 1 of the cards to themselves and the other to the agent (see Fig. 1A). After assignment, the face of both cards became visible for the agent only. The agent was then tasked with informing the recipient about the outcome of the trial by clicking on the card they wanted to assign themselves (see Fig. 1B). Importantly, the agent was expressly informed that, at this point, they could also reverse the outcome of the trial. They could either accept the card they had been assigned or choose the other card, thereby lying about the factual outcome to the recipient. From the agent's perspective, this produced 4 possible outcome conditions: (i) self-serving truth, (ii) self-serving lie, (iii) other-serving truth, and (iv) other-serving lie (see Fig. 1C). Agents made their choice by selecting either the left or right card by pressing the corresponding button on a 2-button response box. Immediately, after their response, the agent received feedback pertaining to the outcome of the trial.

The task consists of a practice block (24 trials) followed by 5 experimental blocks (242 trials in total). Across all experimental blocks, the agents encountered a total of 76 favorable trials (in which they won, unless they lied), and 142 unfavorable trials (in which they lost, unless they lied). The order of favorable and unfavorable trials was counterbalanced across agents. In addition to these decision trials, 25 no-press trials were implemented in which the same card was presented twice. Here, agents were instructed to avoid responding and instead wait for the next trial. These no-press trials were implemented to control for random responses and to ensure alertness throughout.

In each trial, a fixation cross was presented for 1,000 ms, followed by the presentation of 2 cards face-down for 800 ms (see Fig. 2). The cards were presented face-up for 2,500 ms. The card with the bold frame signified the card the recipient had blindly assigned to the agent. The stimulus remained visible on the screen until the agent had given their response, but for a maximum of 2,500 ms. This speed was entrained during the practice block and was well beyond any observed response times during the study. After each trial, the agent received feedback regarding their answer and the trial's outcome ("you told the truth, you won"; "you lied, you won"; "you told the truth, you lost"; "you lied, you lost"), lasting for 2,000 ms. The task itself lasted for ∼30 min.

Procedure

During the task, the agents faced 20 different anonymous recipients who were randomly assigned to the trials. The latter's decisions were prerecorded due to the logistic constraints of the experimental setting. At the end of the task, 3 trials were randomly selected for pay-off. Both players, agent and recipient, were paid real money. Note, participants were fully informed and received detailed instructions pertaining to the nature of the recipients and the experimental task. As such, no cover story was necessary.

For the duration of the experiment, the agents were seated in a sound-, light-, and electrically shielded room to reduce outside influences and to ensure privacy during the task. Communication between the agent and experimenter took place through an intercom connection. Continuous EEG was recorded while agents completed the task. To limit movement artifacts during the EEG recording, agents placed their head on a chinrest for the duration of the task. The experimental blocks were separated by breaks in which agents were instructed to lean back and relax. To record response times accurately, agents provided their answers using a 2-button response box. To ensure privacy and to prevent social desirability effects, experimenters did not know whether or how frequently agents had been dishonest during the task.

Analysis of behavioral data

The main goal of this study was to explain why self-serving lying takes longer than self-serving truth-telling. Thus, we focus only on the agent and only on 2 outcome conditions: self-serving truth and self-serving lie. Self-serving truth will from now on be referred to as Truth and self-serving lie will be referred to as Lie. For each participant (agent), we calculated the mean response time and frequency of occurrence for the trials in which they told the truth to win (Truth condition) and for the trials in which they lied to win (Lie condition) separately. Trials with response times <200 ms or >1,200 ms after stimulus presentation (roughly corresponding to two SDs from the mean response time) were excluded from further analysis (<5.6% of all trials). This time window was chosen to enable group-level analysis by reducing noise and to eliminate trials in which participants did not engage with the task and responded either prematurely or delayed responses.

EEG recording and preprocessing

During the task completion, continuous EEG was recorded using 60 Ag–AgCl electrodes that were mounted in an elastic cap and were placed according to the international 10–10 system
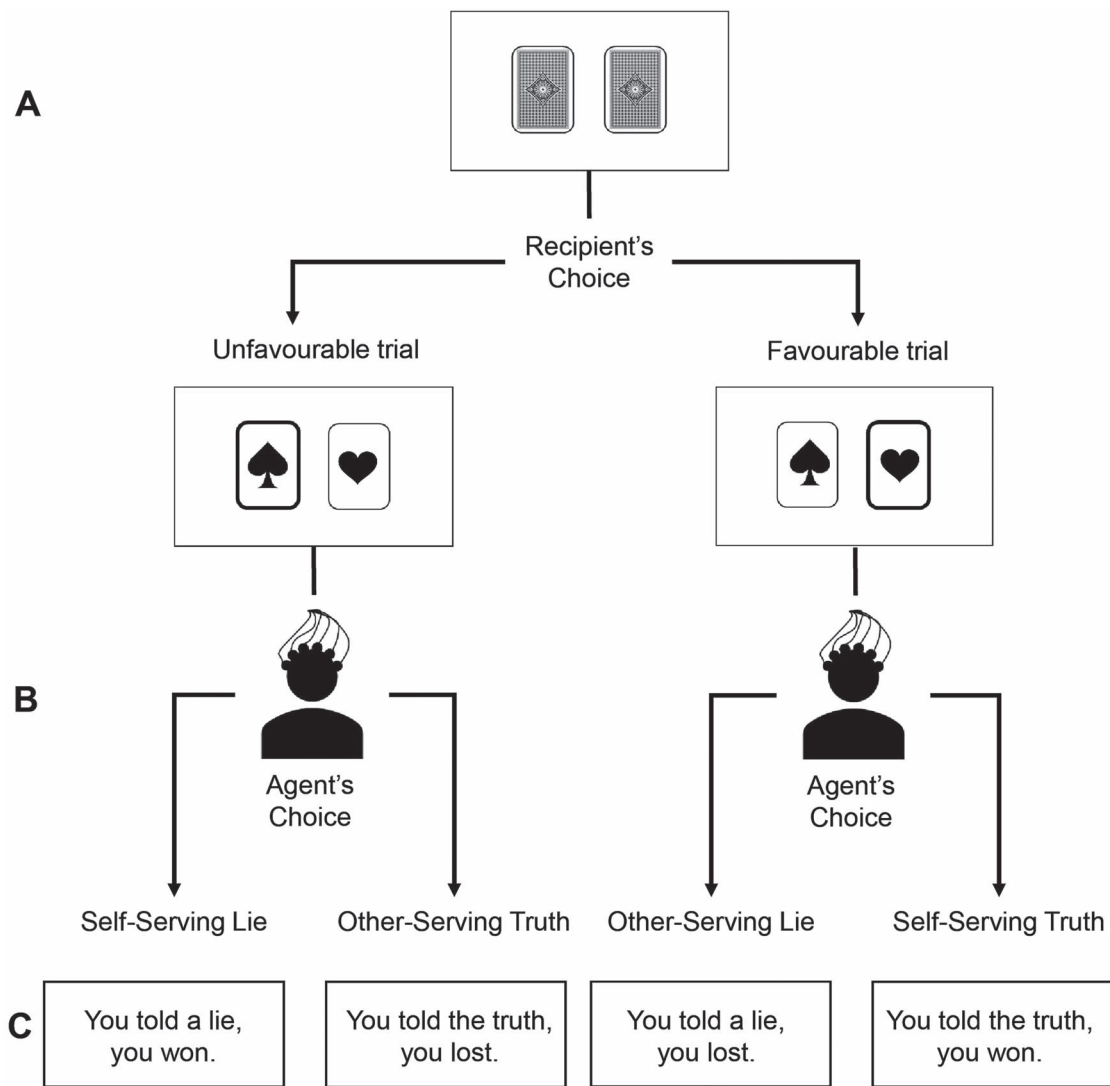
Fig. 1. Illustration of task structure. **A**) The recipient (opponent) makes a blind choice between 2 down-ward facing cards. **B**) The agent (participant) shown here with electrodes can see the initial outcome and can either choose to tell the truth or lie to the recipient. The final outcome of the trial depends on the agent's decision. **C**) Immediately, after their response, the agent received feedback pertaining to the outcome of the trial.
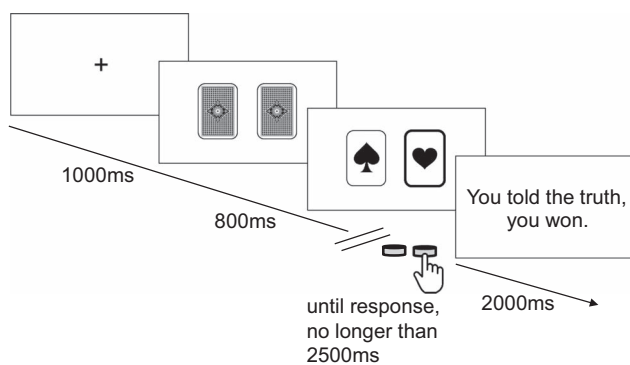
Fig. 2. Illustration of a sample trial in the dishonesty task from the agent's perspective.

(Nuwer et al. 1998). The electrode at position FCz was the recording reference, while the electrode at position CPz served as the ground electrode. Data were recorded at a sampling rate of 500 Hz (bandwidth: 0.1–250 Hz). Horizontal electrooculographic (EOG) signals were recorded at the left and right outer canthi, and vertical EOG signals were recorded below the right eye. Impedances were maintained at <10 kΩ. Eye-movement artifacts were removed using an independent component analysis. After an automatic artifact rejection (maximal allowed voltage step: 15 μV; maximal allowed amplitude: ±100 μV; minimal allowed activity in intervals of 100 ms: 0.5 μV), data were visually inspected to eliminate residual artifacts. Data were then band-pass filtered (high-pass: 1.5 Hz, low-pass: 30 Hz) and were recomputed against the average reference. In order to perform further analyses on the ERPs, for each participant, artifact-free epochs between 200 ms pre-stimulus and 1,000 ms post-stimulus were selected and were baseline-corrected (using a −200 to 0 ms pre-stimulus window as the baseline).

ERP analysis

Using a time window from stimulus onset to 1,000 ms after (which was well beyond the average response times of the 2 conditions), individual artifact-free ERPs were computed for the 2 conditions, Truth and Lie, based on stimulus marker positions (stimulus-locked segmentation). Truth averaged all trials in which

participants told the truth to win the trial. Lie averaged all trials in which participants lied to win the trial. This process was repeated using a time window from button press to 1,000 ms before (response-locked segmentation). To address our research question of why self-serving lying takes longer than self-serving truth-telling, a within-design was used. As such, only participants with a minimum of 30 artifact-free segments in each condition were accepted for further analyses, leaving a sample of 99 participants (69 females and 30 males). Hence, a mean of 69.5 Truth trials (SD = 9.1; minimum = 31) and 97.7 Lie trials (SD = 37.1; minimum = 30) were available for averaging. The individual ERPs were then averaged into 4 grand-mean ERPs, 1 for each respective condition and each segmentation approach: stimulus-locked Truth ERP, stimulus-locked Lie ERP, response-locked Truth ERP, and response-locked Lie ERP.

Combination of segmentation approaches

Behavioral results indicated substantial interindividual variability in response times (see Supplementary Fig. 1). This variability may hinder the effective analysis of late stimulus-locked ERP components (see Supplementary Fig. 2). To circumvent this problem, we decided to combine the stimulus-locked ERP approach with the response-locked ERP approach. To formally determine the point of intersection after which the grand-mean response-locked ERPs provide a better representation of the data, we first need to specify a quantifier that is sensitive to the spatial consistency of ERP scalp potential field maps across participants. Global field power (GFP; Lehmann and Skrandies 1980) of the grand-mean ERP maps across participants is highly suitable to serve as this quantifier. This is because, the GFP of the grand-mean ERP map (mean map across all participants at 1 time point) depends not only on the amplitude of the individual maps but also on the spatial consistency of these maps across participants. If there are more spatially consistent activities across participants, the GFP of the grand-mean ERP map is high (see Supplementary Fig. 2B). By contrast, if there are substantial differences in the individual maps, the potential values are canceled out during the computation of the grand-mean ERP map, and as a result, the GFP of the grand-mean ERP map is low. We can, therefore, state that the GFP of the grand-mean ERP map depends systematically on the consistency of active sources across all participants.

Microstate analysis

To identify sequences of time periods with quasi-stable scalp map topographies referred to as functional microstates (Lehmann and Skrandies 1980; Lehmann 1987), the spatial K-means clustering approach was used (Pascual-Marqui et al. 1995; Koenig and Melie-García 2010, for alternative approaches, see Cacioppo et al. 2014). This strategy uses global map dissimilarity (Lehmann and Skrandies 1980) as a measure of topographical difference between any 2 maps. Spatial cluster analysis allowed us to define the most dominant topographies (i.e. clusters) in the grand-mean stimulus-locked ERP map series of the Truth and the Lie conditions on the whole time period, that is, from stimulus onset to 1,000 ms after. In order to define the optimal number of clusters, models with varying numbers of clusters were computed over a subset of data (training data). And, averaged over the remaining participants (test data), the models were then examined for their mean correlation in stimulus-locked ERPs. This procedure was repeated 50 times. For each model, the mean correlation of test data with the model was averaged across the results obtained in the different subsets. This allows for the model to be complex enough to accommodate for between-participant variance, while

reducing within-participant variance (for a detailed description of this procedure, see Koenig et al. 2014). The number of clusters that best explained the group-averaged data was chosen (Koenig et al. 2011, 2014).

We then applied a topographical fitting procedure to identify the resulting microstates in each of the grand-mean stimulus-locked ERP up to the respective point of intersection (e.g. Michel et al. 1999). We applied the constraint that a given cluster must be observed for at least 10 consecutive time points (>20 ms) in the grand-mean stimulus-locked ERP. This fitting procedure gave us the onset and offset of each microstate in each grand-mean stimulus-locked ERP up to the respective point of intersection. Clustering and fitting procedures were repeated using grand-mean response-locked ERPs for the remaining time period, from the intersection point of the GFP curves for stimulus- and response-locked ERPs until the average time of button press, together for the Lie and the Truth conditions. Analyses were conducted in Randomization Graphical User interface (Koenig et al. 2011).

Source localization

We sought to estimate the intracerebral sources that likely gave rise to each of the microstates by using the standardized low-resolution brain electromagnetic tomography (sLORETA, Pascual–Marqui 2002). The sLORETA algorithm has been widely used in many EEG studies (Knoch et al. 2010; Murphy and Dacin 2011; Schiller et al. 2016). This method has been shown to outperform several other linear inverse algorithms (Pascual-Marqui 2002) and has been extensively crossvalidated (for details, see Supplementary Methods).

Results
## Lying takes longer than truth-telling

On average, participants took significantly longer to lie (*M* = 759.5 ms, SD = 133.6 ms) than to tell the truth (*M* = 702.1 ms, SD = 103.9 ms; [*t*(98) = 8.32, *P* < 0.0001, *d* = 0.83]; see Supplementary Fig. 1). The average difference in response times between Lie and Truth was 57.3 ms (SD = 68.3 ms). The expected response time effect was observed.

Why does lying take longer than truth-telling?

The intersection of the grand-mean GFP time series for stimulus- and response-locked ERPs indicates the time point after which the grand-mean response-locked ERPs provide a better representation of the data. For the Truth condition, the intersection point corresponds to 478 ms after the stimulus onset and to 224 ms before the average response time, whereas for the Lie condition, the intersection point corresponds to 538 ms after the stimulus onset and to 222 ms before the average response time (see Supplementary Fig. 3). A paired *t*-test confirmed that individuals' intersection points in the Lie condition were significantly later compared to the Truth condition [*t*(98) = 3.01, *P* = 0.003, *d* = 0.30].

Combination of stimulus- and response-locked ERPs revealed 7 clusters—that is, to say the 7 most dominant topographies (see Fig. 3A): 5 clusters based on stimulus-locked ERPs up to point of intersection (a total of 6 clusters were found from stimulus-locked ERPs to 1,000 ms after), and 2 clusters based on response-locked ERPs from point of intersection to button press. Fitting the clusters to each stimulus-locked or response-locked grand-mean ERP, respectively, by means of spatial correlation demonstrated a sequence of 6 microstates—representing the implementation of distinct mental states—in the Truth condition,
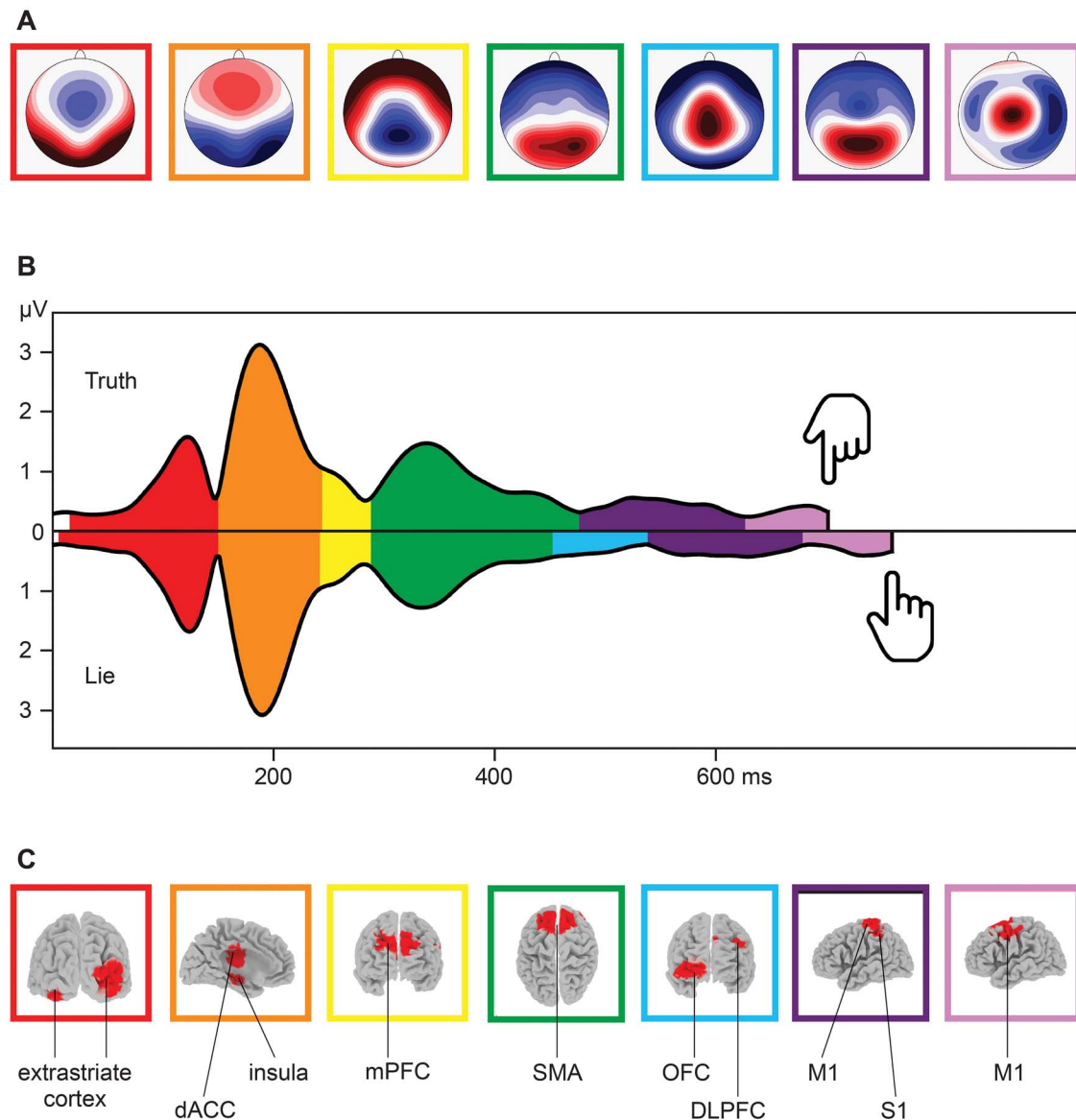
Fig. 3. Stimulus- and response-locked microstate analysis of dishonesty task related ERPs. **A**) Topographies of the 7 clusters in the sequence of occurrence. Head seen from above: Red indicates positive values and blue indicates negative values, referred to average reference. The colored frame corresponds to the assignment shown in B and C. **B**) Stimulus- and response-locked microstates across time for the Truth (upper) and Lie conditions (lower) plotted over GFP. Colors refer to the microstate topographies shown in A. The hand symbols indicate mean response times. The vertical axis indicates GFP (in microvolts); the horizontal axis indicates time (in milliseconds). **C**) Localization of the intracortical sources as estimated with sLORETA for the full sequence of microstates during the dishonesty task. The best 25% of the voxels are colored in red. We labeled the main activation clusters and framed the localization with the same color code as the corresponding microstates in A and B. dACC, dorsal anterior cingulate cortex; mPFC, medial prefrontal cortex; OFC, orbitofrontal cortex; M1, primary motor cortex; S1, primary somatosensory cortex.

and 7 microstates in the Lie condition (see Fig. 3B and Table 1). This suggests that the observed between-condition response time differences can be explained by the occurrence of an additional microstate, microstate 5 (454–536 ms) in the Lie condition.

We additionally examined our data for the differences in duration between the microstates present in both conditions. We found that one microstate, microstate 4 (starting around 290 ms) was prolonged in the Truth condition ($M_{Truth} = 186$ ms; $M_{Lie} = 162$ ms, $P < 0.001$; Fig. 3B and Table 1). Taken together, these findings suggest that the observed response time differences are a result of both an additional microstate during dishonest responses and a prolonged microstate during honest responses.

Source localization

In a final step, we source localized both microstates 4 and 5 to get an idea about the nature of these processes which appear to account for the prolonged response times in the Lie condition (Fig. 3C; for a detailed description of source localization results of all microstates, see Supplementary Results and Supplementary Table 1). Microstate 4 was characterized by the activity in the supplementary motor area (SMA; BA6). Microstate 5 was characterized by the activity in the dorsolateral prefrontal cortex (DLPFC, BA9) and the orbitofrontal cortex (OFC; BA10/11).

Discussion

This study sought to understand why self-serving dishonesty takes longer than self-serving honesty. Much of the existing literature indicates that lying is more cognitively demanding than truth-telling (e.g. Zuckerman et al. 1981; Sporer and Schwandt 2006, 2007; Vrij et al. 2010; Walczyk et al. 2014; Debey et al. 2015). How these increased cognitive demands are expressed, however,

Table 1. Descriptive onsets and offsets of microstates in milliseconds.

Microstate	1 On		Off	2 On		Off	3 On		Off	4 On		Off	5 On		Off	6 On		Off	7 On		Off
Truth	0	–	150	152	–	244	246	–	288	290	–	476	-		-	478	–	626	628	–	702
Lie	0	–	150	152	–	242	244	–	288	290	–	452	454	–	536	538	–	678	680	–	760

is—as yet—unclear. Does an additional mental process occur during dishonest decision-making or do participants simply take longer to execute 1 or multiple mental processes when telling a lie?

To answer this question, we contrasted spontaneous self-serving honest and dishonest behavior using a data-driven, spatiotemporal EEG microstate approach. To study mental processes in real time, it is critical to use a method that offers sufficiently sensitive temporal resolution, such as EEG. Numerous studies have attempted to unravel the mental processes underlying dishonesty using ERPs (Johnson et al. 2003; Rosenfeld et al. 2003; Wu et al. 2009; Hu et al. 2011; Proverbio et al. 2013; Panasiti et al. 2014; Zhu et al. 2019). These have provided valuable insights into dishonesty and have focused on the specific elements of dishonesty, such as the role of cognitive control in dishonesty (e.g. Johnson et al. 2008; Carrión et al. 2010), the content of the dishonest expression (Hu et al. 2011), and various lie detection paradigms (Proverbio et al. 2013; Pfister et al. 2014; Rosenfeld 2020) and have highlighted the role of specific characteristic ERPs involved in dishonest decision-making. While these studies capitalize on the high temporal resolution of EEG, they generally preselect both the time period and channels that are to be analyzed. This limits the scope of the insights provided by these studies to the specific time and spatial window investigated. As such, they cannot answer the question of why lying takes longer than truth-telling, as they cannot provide a complete overview of the entire chain of mental processes unlike the approach adopted here. We, therefore, extend and integrate the classical ERP analysis by providing a comprehensive global, big picture perspective.

The comprehensive microstate analysis procedure adopted in our study, combined with source localization, enabled us to identify and contrast the complete chronology of mental processes involved during self-serving honesty and dishonesty. From stimulus onset until response implementation, we identified 6 mental processes during honesty and 7 mental processes during dishonesty. That is to say, we did, in fact, observe an additional late occurring mental process (microstate 5; 454–536 ms) when participants told a lie.

However, we did not observe any mental processes with prolonged duration during dishonest responses. As such, it appears that an additional mental process, microstate 5, underlies the response time difference between dishonesty and honesty. Unexpectedly, the preceding microstate, microstate 4, had a significantly shorter duration during dishonesty (290–452 ms) compared to honesty (290–476 ms), indicating that participants were faster to execute this mental process during a lie. Despite initially seeming counterintuitive, the fact that this shortened microstate appears immediately prior to the microstate uniquely characterizing dishonesty is crucial to interpreting these findings.

So, what can we tell about these 2 processes? Building on the results of source localization coupled with information about the time and order of appearance of these 2 microstates, we were able to make some inferences regarding the mental processes taking place. Source localization of microstate 4 revealed activity in the SMA (BA6), suggesting that this process is related to participants selecting their motor response (e.g. Fried et al. 1991). Microstate 5 was characterized by the activity in the DLPFC (BA9)—thought to be critical for control and response inhibition (e.g. MacDonald et al. 2000; Miyake et al. 2000; Miller and Cohen 2001; Oldrati et al. 2016) and the orbitofrontal cortex (OFC; BA10/11). The OFC is part of the so-called brain valuation system (e.g. Rangel et al. 2008), a neural network involved in the valuation and processing of rewards (e.g. Ruff and Fehr 2014; Padoa-Schioppa and Conen 2017; Lopez-Persem et al. 2020). Based on the order of appearance and their pattern of neural activation, we speculate that, when participants are dishonest, the response implemented in microstate 4 is evaluated and inhibited, thereby cutting its duration short. As such, microstate 5 only comes into play when participants decide to lie, interrupting the response selection processes taking place in microstate 4.

Taken together, it thus appears that prolonged response times during dishonesty are a result of 1 shortened microstate and 1 additionally occurring microstate. These findings provide evidence in support of the cognitive approach to dishonesty. This postulates that lying is more cognitively demanding than truth-telling (e.g. Debey et al. 2014). To execute a lie, the truth is first activated before it is subsequently inhibited (e.g. Duran et al. 2010; Walczyk et al. 2014; Debey et al. 2015). This dualistic character of dishonesty is nicely reproduced in the initial activation of the truth in microstate 4 and its subsequent inhibition in microstate 5 as outlined above.

When considering the present findings in the context of the existing research, there is 1 other crucial aspect to consider: the ecological validity of the task that was used. In contrast to other tasks (for an overview of frequently employed tasks, see Gerlach et al. 2019), the "temptation to lie" game is comparatively ecologically valid as it fulfills three key characteristics: (i) Lying is spontaneous, not instructed; (ii) deceit is detrimental to a social partner, and (iii) decisions have real monetary consequences for both parties. Many previous studies that have found evidence in support of the deception-related cognitive conflict have relied on explicitly instructing participants to lie (e.g. Seth et al. 2006; Sip et al. 2008; Ganis and Keenan 2009; Carrión et al. 2010). Instead, the dishonest behavior exhibited in this dishonesty task seems to more credibly relay realistic day-to-day dishonesty. Moreover, the design adopted here overcomes 1 more crucial limitation of existing paradigms in that dishonesty can be directly observed and can be detected on a trial-by-trial basis without compromising the ecological validity of the task—rather than indirectly inferred as is the case in commonly employed "roll of a dice" tasks (e.g. Fischbacher and Föllmi-Heusi 2013).

Finally, the analysis presented here differs from existing work where Lie and Truth are often confounded with other-serving and self-serving motives. Although participants in our paradigm did have to choose between self-serving and other-serving outcomes,

thereby reflecting real-life spontaneous dishonesty—focusing our analysis on the self-serving conditions only, we were able to successfully isolate what differentiates Lie and Truth when the outcome (win) itself is held constant.

The microstate approach adopted here has potential to illuminate the chronometry of mental processes involved in social and economic decision-making paradigms and cognitive processes more generally. For example, building on existing neuroeconomic theories conceiving dishonesty as a cost–benefit trade-off (e.g. Brocas and Carrillo 2019), it is reasonable to assume that similar mental processes take place during decision-making relating to other moral transgressions or illegal actions, such as free-riding and corruption. We thus encourage others to adopt the approach presented here and hope to have clarified that focusing on preselected time windows—while providing valuable insights—limits the scope of possible findings in the study of the psychological sources of response time differences in a variety of contexts.

Conclusion

To conclude, the spatiotemporal approach adopted here allowed for an integrative holistic analysis of all mental processes from the stimulus onset to response rather than specific time windows. Only by adopting this comprehensive approach, we could determine why lying takes longer than truth-telling. In this study, we found that the observed response time differences between lying and truth-telling were due to an additional microstate during dishonesty, which impeded on and thereby shortened and attenuated the preceding process of response selection. We were thus able to reconcile the preexisting findings of neuroimaging and behavioral studies comparing honesty and dishonesty.

Acknowledgements

Supplementary material

Supplementary material is available at *Cerebral Cortex* online.

Funding

Data availability

All data, code, and materials are available at: https://github.com/lorenarrgianotti/ThePathOfDishonesty upon publication.

References

Abe N, Suzuki M, Tsukiura T, Mori E, Yamaguchi K, Itoh M, Fujii T. Dissociable roles of prefrontal and anterior cingulate cortices in deception. *Cereb Cortex*. 2006:16:192–199.

Azevedo RT, Panasiti MS, Maglio R, Aglioti SM. Perceived warmth and competence of others shape voluntary deceptive behaviour in a morally relevant setting. *Br J Psychol*. 2018:109:25–44.

Bressler SL. Large-scale cortical networks and cognition. *Brain Res Rev*. 1995:20:288–304.

Brocas I, Carrillo JD. A neuroeconomic theory of (dis) honesty. *J Econ Psychol*. 2019:71:4–12.

Cacioppo S, Weiss RM, Birali H, Cacioppo JT. Dynamic spatiotemporal brain analyses using high performance electrical neuroimaging: theoretical framework and validation. *J Neurosci Methods*. 2014:238:11–34.

Carrión RE, Keenan JP, Sebanz N. A truth that's told with bad intent: an ERP study of deception. *Cognition*. 2010:114:105–110.

Debey E, De Houwer J, Verschuere B. Lying relies on the truth. *Cognition*. 2014:132:324–334.

Debey E, Ridderinkhof RK, De Houwer J, De Schryver M, Verschuere B. Suppressing the truth as a mechanism of deception: delta plots reveal the role of response inhibition in lying. *Conscious Cogn*. 2015:37:148–159.

DePaulo BM. The many faces of lies. In: Miller AG, editors. *The social psychology of good and evil*. New York: Guilford Press; 2004. pp. 303–326.

Duran ND, Dale R, McNamara DS. The action dynamics of overcoming the truth. *Psychon Bull Rev*. 2010:17:486–491.

Engelmann JB, Fehr E. The slippery slope of dishonesty. *Nat Neurosci*. 2016:19:1543–1544.

Fischbacher U, Föllmi-Heusi F. Lies in disguise-an experimental study on cheating. *J Eur Econ Assoc*. 2013:11:525–547.

Fried I, Katz A, McCarthy G, Sass KJ, Williamson P, Spencer SS, Spencer DD. Functional organization of human supplementary motor cortex studied by electrical stimulation. *J Neurosci*. 1991:11: 3656–3666.

Fuster JM. The cognit: a network model of cortical representation. *Int J Psychophysiol*. 2006:60:125–132.

Gächter S, Schulz JF. Intrinsic honesty and the prevalence of rule violations across societies. *Nature*. 2016:531:496–499.

Ganis G, Keenan JP. The cognitive neuroscience of deception. *Soc Neurosci*. 2009:4:465–472.

Gerlach P, Teodorescu K, Hertwig R. The truth about lies: a meta-analysis on dishonest behavior. *Psychol Bull*. 2019:145:1–44.

Heyneman SP, Anderson KH, Nuraliyeva N. The cost of corruption in higher education. *Comp Educ Rev*. 2008:52:1–25.

Hu X, Wu H, Fu G. Temporal course of executive control when lying about self- and other-referential information: an ERP study. *Brain Res*. 2011:1369:149–157.

Johnson R, Barnhardt J, Zhu J. The deceptive response: effects of response conflict and strategic monitoring on the late positive component and episodic memory-related brain activity. *Biol Psychol*. 2003:64:217–253.

Johnson R, Henkell H, Simon E, Zhu J. The self in conflict: the role of executive processes during truthful and deceptive responses about attitudes. *NeuroImage*. 2008:39:469–482.

Kahneman D. *Thinking, fast and slow*. London: Macmillan; 2011.

Knoch D, Gianotti LRR, Baumgartner T, Fehr E. A neural marker of costly punishment behavior. *Psychol Sci*. 2010:21:337–342.

Koenig T, Melie-García L. A method to determine the presence of averaged event-related fields using randomization tests. *Brain Topogr*. 2010:23:233–242.

Koenig T, Kottlow M, Stein M, Melie-García L. Ragu: a free tool for the analysis of EEG and MEG event-related scalp field data using global randomization statistics. *Comput Intell Neurosci*. 2011:1–15.

Koenig T, Stein M, Grieder M, Kottlow M. A tutorial on data-driven methods for statistically assessing ERP topographies. *Brain Topogr*. 2014:27:72–83.

Kruglanski AW, Gigerenzer G. Intuitive and deliberate judgments are based on common principles. *Psychol Rev*. 2011:118:97–109.

Lehmann D. Principles of spatial analysis. In: Gevins AS, Remont A, editors. editors*Methods of analysis of brain electrical and magnetic signals*. Amsterdam: Elsevier; 1987. pp. 309–354

Lehmann D, Skrandies W. Reference-free identification of components of checkerboard-evoked multichannel potential fields. *Electroencephalogr Clin Neurophysiol*. 1980:48:609–621.

Lopez-Persem A, Bastin J, Petton M, Abitbol R, Lehongre K, Adam C, Navarro V, Rheims S, Kahane P, Domenech P et al. Four core properties of the human brain valuation system demonstrated in intracranial signals. *Nat Neurosci*. 2020:23:664–675.

MacDonald AW, Cohen JD, Stenger VA, Carter CS. Dissociating the role of the dorsolateral prefrontal and anterior cingulate cortex in cognitive control. *Science*. 2000:288:1835–1838.

Maréchal MA, Cohn A, Ugazio G, Ruff CC. Increasing honesty in humans with noninvasive brain stimulation. *Proc Natl Acad Sci U S A*. 2017:114:4360–4364.

Mauro P. Corruption and growth. *Q J Econ*. 1995:110:681–712.

Mesulam MM. From sensation to perception. *Brain*. 1998:121: 1013–1052.

Michel CM, Brandeis D, Skrandies W, Pascual R, Strik WK, Dierks T, Hamburger HI, Karniski W. Global field power: a "time-honoured" index for EEG/EP map analysis. *I J Psychophysiol*. 1993:15:1–2.

Michel CM, Seeck M, Landis T. Spatiotemporal dynamics of human cognition. *News Physiol Sci*. 1999:14:206–214.

Miller EK, Cohen JD. An integrative theory of prefrontal cortex function. *Annu Rev Neurosci*. 2001:24:167–202.

Miyake A, Friedman NP, Emerson MJ, Witzki AH, Howerter A, Wager TD. The unity and diversity of executive functions and their contributions to complex "frontal lobe" tasks: a latent variable analysis. *Cogn Psychol*. 2000:41:49–100.

Murphy PR, Dacin MT. Psychological pathways to fraud: understanding and preventing fraud in organizations. *J Bus Ethics*. 2011:101: 601–618.

Nuwer MR, Comi G, Emerson R, Fuglsang-Frederiksen A, Guérit JM, Hinrichs H, Ikeda A, Luccas FJ, Rappelsburger P. IFCN standards for digital recording of clinical EEG. *Electroencephalogr Clin Neurophysiol*. 1998:106:259–261.

Oldrati V, Patricelli J, Colombo B, Antonietti A. The role of dorsolateral prefrontal cortex in inhibition mechanism: a study on cognitive reflection test and similar tasks through neuromodulation. *Neuropsychologia*. 2016:91:499–508.

Padoa-Schioppa C, Conen KE. Review orbitofrontal cortex: a neural circuit for economic decisions. *Neuron*. 2017:96:736–754.

Panasiti MS, Pavone EF, Merla A, Aglioti SM. Situational and dispositional determinants of intentional deceiving. *PLoS One*. 2011:6: 2–7.

Panasiti MS, Pavone EF, Mancini A, Merla A, Grisoni L, Aglioti SM. The motor cost of telling lies: electrocortical signatures and personality foundations of spontaneous deception. *Soc Neurosci*. 2014:9:573–589.

Panasiti MS, Cardone D, Pavone EF, Mancini A, Merla A, Aglioti SM. Thermal signatures of voluntary deception in ecological conditions. *Sci Rep*. 2016:6:1–10.

Pascual-Marqui RD. Standardized low resolution brain electromagnetic tomography. *Methods Find Exp Clin Pharmacol*. 2002: 24:5–12.

Pascual-Marqui RD, Michel CM, Lehmann D. Segmentation of brain electrical activity into microstates; model estimation and validation. *IEEE Trans Biomed Eng*. 1995:42:658–665.

Pfister R, Foerster A, Kunde W. Pants on fire: the electrophysiological signature of telling a lie. *Soc Neurosci*. 2014:9:562–572.

Proverbio AM, Vanutelli ME, Adorni R. Can you catch a liar? How negative emotions affect brain responses when lying or telling the truth. *PLoS One*. 2013:8:e59383.

Rangel A, Camerer C, Montague PR. A framework for studying the neurobiology of value-based decision making. *Nat Rev Neurosci*. 2008:9:545–556.

Rosenfeld JP. P300 in detecting concealed information and deception: a review. *Psychophysiology*. 2020:57:e13362.

Rosenfeld JP, Rao A, Soskins M, Reinhart MA. Scaled P300 scalp distribution correlates of verbal deception in an autobiographical oddball paradigm: control for task demand. *J Psychophysiol*. 2003:17:14–22.

Ruff CC, Fehr E. The neurobiology of rewards and values in social decision making. *Nat Rev Neurosci*. 2014:15:549–562.

Schiller B, Gianotti LRR, Baumgartner T, Nash K, Koenig T, Knoch D. Clocking the social mind by identifying mental processes in the IAT with electrical neuroimaging. *Proc Natl Acad Sci U S A*. 2016:113:2786–2791.

Seth AK, Iversen JR, Edelman GM. Single-trial discrimination of truthful from deceptive responses during a game of financial risk using alpha-band MEG signals. *NeuroImage*. 2006:32:465–476.

Shalvi S, Eldar O, Bereby-Meyer Y. Honesty requires time and lack of justifications. *Psychol Sci*. 2012:23:1264–1270.

Sip KE, Roepstorff A, McGregor W, Frith CD. Detecting deception: the scope and limits. *Trends Cogn Sci*. 2008:12:48–53.

Speer SPH, Smidts A, Boksem MAS. Cognitive control increases honesty in cheaters but cheating in those who are honest. *Proc Natl Acad Sci U S A*. 2020:117:19080–19091.

Sporer SL, Schwandt B. Paraverbal indicators of deception: a meta-analytic synthesis. Applied cognitive psychology. *J Appl Res Mem Cogn*. 2006:20:421–446.

Sporer SL, Schwandt B. Moderators of nonverbal indicators of deception: a meta-analytic synthesis. *Psychol Public Policy Law*. 2007:13: 1–34.

Suchotzki K, Verschuere B, Bockstaele B, Van Ben-Shakhar G, Crombez G. Lying takes time: a meta-analysis on reaction time measures of deception. *Psychol Bull*. 2017:14:428–453.

Tanzi V, Davoodi H. Corruption, public investment, and growth. In: *The welfare state, public investment, and growth*. Japan: Springer; 1998. pp. 41–60

Vrij A, Granhag PA, Porter S. Pitfalls and opportunities in nonverbal and verbal lie detection. *Psychol Sci Public Interest*. 2010:11:89–121.

Walczyk JJ, Harris LL, Duck TK, Mulay D. A social-cognitive framework for understanding serious lies: activation-decision-construction-action theory. *New Ideas Psychol*. 2014:34: 22–36.

Wu H, Hu X, Fu G. Does willingness affect the N2-P3 effect of deceptive and honest responses? *Neurosci Lett*. 2009:467:63–66.

Zhu C, Pan J, Li S, Liu X, Wang P, Li J. Internal cost of spontaneous deception revealed by ERPs and EEG spectral perturbations. *Sci Rep*. 2019:9:1–11.

Zuckerman M, DePaulo BM, Rosenthal R. Verbal and nonverbal communication of deception. *Adv Exp Soc Psychol*. 1981:14: 1–59.